MRI and histologic studies on early markers of Alzheimer's disease

Duijn, S. van

Chapter 3

Comparison of histological techniques to visualize iron in paraffin embedded brain tissue of patients with Alzheimer's disease.

Sara van Duijn, MSc 1, Rob J.A. Nabuurs, MD, PhD 2, Sjoerd G. van Duinen, MD, PhD 1, Remco Natté, MD, PhD 1

1. Department of Pathology, Leiden University Medical Centre, Leiden, Netherlands
2. Department of Radiology, Leiden University Medical Centre, Leiden, Netherlands

J. Histochem. Cytochem. 2013 Nov; 61 (11): 785-792

Abstract

Better knowledge of the distribution of iron in the brains of Alzheimer's disease (AD) patients may facilitate the development of an in vivo magnetic resonance (MR) marker for AD and may cast light on the role of this potentially toxic molecule in the pathogenesis of AD. Several histological iron staining techniques have been used in the past but they have not been systematically tested for sensitivity and specificity.

This article compares three histochemical techniques and ferritin immunohistochemistry to visualize iron in paraffin embedded human AD brain tissue. The specificity of the histochemical techniques was tested by staining sections after iron extraction.

Iron was demonstrated in the white matter, in layers IV/V of the frontal neocortex, in iron containing plaques, and in microglia. In our hands these structures were best visualized using the Meguro iron stain, a method that has not been described for iron staining in human brain or AD in particular. Ferritin immunohistochemistry stained microglia and iron containing plaques similar to the Meguro method but was less intense in myelin associated iron. The Meguro method is most suitable for identifying iron positive structures in paraffin-embedded human AD brain tissue.

Keywords: iron, Alzheimer's disease, ferritin, brain, plaques, microglia

Introduction

There is growing evidence that iron plays an important role in the development of neurodegenerative diseases such as Alzheimer's disease (AD). One of the reasons is an altered brain iron distribution with iron accumulation in AD plaques (LeVine 1991; Smith et al. 1997; Crichton et al. 2002; Haacke et al. 2005; Meadowcroft et al. 2009; Bartzokis 2011). These disease-related changes in brain iron distribution are a potential marker for early in vivo diagnosis using MRI, especially because recent advances in human magnetic resonance imaging (MRI), systems operating at an ultra-high magnetic field (7 Tesla and higher) show increased sensitivity to iron-based susceptibility contrast in the human brain that have not been observed before (Nabuurs et al. submitted). A validated histological method to stain iron in brain tissue is required to correlate the MRI findings with histological changes in iron distribution and to study the role of iron in the development of neurodegenerative diseases like AD.

Iron (Fe) is essential for the proper functioning of many cellular processes. Due to its capability to catalyze oxidation-reduction reactions, iron serves as an active site in molecules with critical biological functions. However, this also requires a strict regulation to prevent uncontrolled spreading of catalytic active iron and its potential (neuro) toxicity (Meguro et al. 2007). This regulation is achieved by strong binding between iron and the proteins transferrin and ferritin. Transferrin, a transporter protein, can bind two Fe3+ ions. Ferritin serves as the principle iron storage protein capable of binding up to 4500 iron atoms in different mineral forms, predominantly as Fe3+ and small amounts of Fe2+ (Meguro et al. 2007). In organisms iron can be categorized as heme or non-heme iron. Heme iron is a Fe2+ protoporphyrin complex found in, for instance, haemoglobin. Non-heme iron consists of Fe3+ bound to ferritin or transferrin and very small amounts of Fe3+ and Fe2+ loosely bound to organic bases, enzymes, iron sulphur proteins and nucleotides. In general, nearly all non-heme iron found in the human body is bound to ferritin as Fe3+. The distribution of ferritin closely resembles the distribution of iron and therefore may act as a surrogate marker for iron (Grundke-Iqbal et al. 1990;Meguro et al. 2007).

In the normal brain, most iron is present in myelin and oligodendrocytes which require irondependent enzymes to produce and maintain myelin. Myelin-rich areas such as white matter thus contain large amounts of iron. In the cerebral cortex, iron is also expected in the myelin-rich layers

IV and V (Fatterpekar et al. 2002). In damaged brain tissue, microglial cells have been shown to accumulate iron (Schonberg et al. 2012).
Non-heme iron (predominantly in the Fe3+ form) can be visualized in paraffin embedded tissue by the classic Perl's iron stain, in which soluble ferrocyanide reacts with the tissue Fe3+ to form crystals that make an insoluble Prussian blue dye. Further enhancement can be obtained by allowing the Prussian blue crystal to catalyze the H2O2-dependent oxidation of diaminobenzidine (DAB) (Meguro et al. 2007). Several protocols for DAB-enhanced iron stains, using different pre-treatment, slide thickness, endogenous blocking and reagent concentrations have been published but these different methodologies have never been directly compared with one and another and only some staining patters have been related to ferritin immunohistochemistry (IHC) (Barbeito et al. 2009; Butt et al. 2010; Fukunaga et al. 2010; Chen-Roetling et al. 2011; Shpyleva et al. 2011) or checked for false positive results in iron depleted sections (Smith et al. 2007). The DAB enhanced histochemical iron stains described by Smith (Smith et al. 1997) and LeVine (LeVine 1991) have been reported to label AD plaques. The Meguro method (Meguro et al. 2007) has not been described in human brain tissue or animal models of AD but has been widely used in other organs in rat, mice and monkey (Meguro et al. 2005; Meguro et al. 2007; Freret et al. 2008; Iwatsuki et al. 2008; Meguro et al. 2008; Butt et al. 2010;Winter et al. 2010; Butt et al. 2011; Shpyleva et al. 2011).
The purpose of the present study is to compare the Meguro, Smith, and LeVine iron staining methods for detection of non-heme iron in brain tissue with AD pathology. In addition, we investigated their correlation with the distribution of ferritin by IHC.

Materials and methods

Brain tissue samples

One block of formalin-fixed, paraffin embedded brain tissue of the frontal cortex of 4 AD patients (60-87 y; Braak 6: N = 2; Braak 5: N = 1; Braak 4: N = 1) and 4 control patients without dementia of evidence of AD (62-76 y; Braak 0) was used. Samples were handled in a coded fashion to maintain anonymity according to Dutch national ethical guidelines. The brain tissue had been routinely immersed in buffered 10% formalin for a maximum of 6 months.

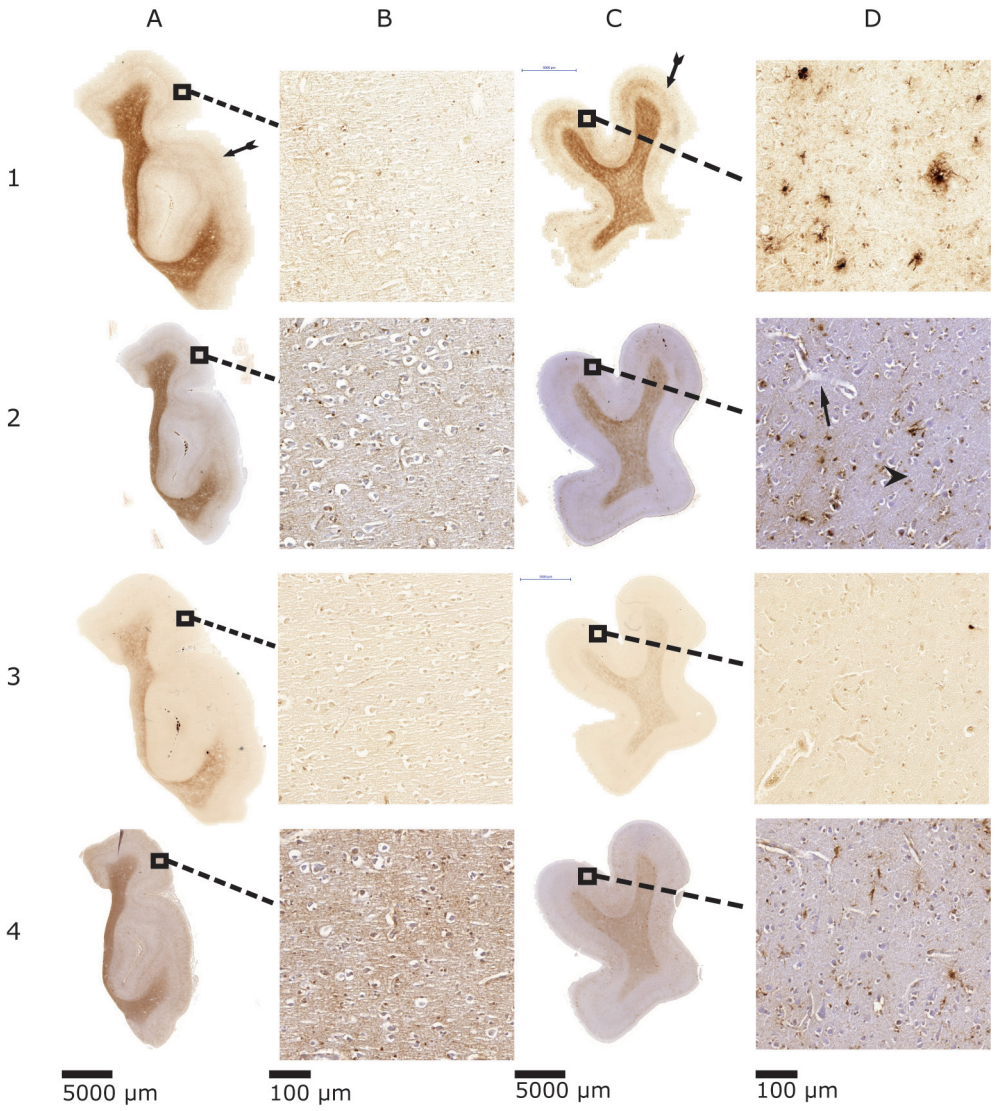

Figure 1: Comparison of the Meguro (1), Smith (2), LeVine (3) and ferritin IHC (4) in control patients (A and B) and AD patients (C and D). A: whole section of a control patient (scale bar 5000 µm); B: 20x magnification of A (scale bar 100 µm); C: whole section of an AD patient (scale bar 5000 µm); D: 20x magnification of C (scale bar 100 µm). Arrows indicate examples of iron positive plaques; arrowheads indicate examples of microglia; double arrows show layer IV/V of the cortex.

Iron extraction

In the first experiment, the tissue of AD patients was used to examine the effect of iron extraction on the different stainings. For each patient

sample 7 serially cut 10 µm thick sections were mounted onto slides. Of each of these series, section 1, 3 and 5 were incubated with 250 µl 0,1 M Na-citrate/HCL pH 1,0 buffer (Boom BV, Meppel, The Netherlands). After overnight incubation, the buffer was aspirated from the section and its iron concentration was measured using the Cobas Integra 400/800 method (Roche Diagnostics, Mannheim, Germany). As a control, the iron concentration was tested in the native buffer, in buffer incubated on a glass slide without tissue and in buffer with Fe3+ (Menck BV, Amsterdam, The Netherlands) added as a positive control. The limits of sensitivity of the Fe elution assay are 0,9-179 µmol/L (Roche Diagnostics).
As a control experiment the tissue of AD patients was used to test the iron extraction capability of Na-citrate/HCL buffer. Of each patient sample a section was incubated with 250 µl 0,05 M TRIS/HCL pH 1,0 buffer (Menck BV) and an adjacent section was incubated with 250 µl 0,1 M Na-citrate pH 1,0 buffer to extract iron. After overnight incubation, the buffer was aspirated from the section and its iron concentrations was measured as described above.

Histological procedures for iron staining
For the first experiment, the sections of AD tissue as described above were used. Of each patient sections 1 and 2 were stained as described by Meguro et al. (Meguro et al. 2007) with an increase in incubation times of 25%: after de-waxing/rehydration the paraffin sections were incubated for 40 min in 1% potassium ferrocyanide, washed and treated in methanol containing 0.01 M NaN3 and 0,3% H2O¬2 for 75 min. Then the sections were treated in 0.1 M phosphate buffer, followed by a solution containing 0.025% 3,3'-DAB-4HCL (DAB, Sigma, St Louis, MO, USA) and 0.005% H2O2 in a 0.1 M phosphate buffer for 40 min. The reaction was stopped by washing.
The third and fourth sections were stained according to Smith et al. (Smith et al., 1997) In short, after deparaffinization in xylene and rehydration through graded ethanol, sections were incubated for 15 hrs in 7% potassium ferrocyanide in aqueous hydrochloric acid (3%) and subsequently incubated in 0.075 % 3,3'-DAB and 0.015% H2O2 for 5–10 min.
The fifth and sixth sections were stained according to Levine et al. (LeVine 1991) but with an increased DAB incubation time of 1 hour and 45 minutes. Briefly, after deparaffinization and rehydration the sections were incubated in 10 mg NaBH4/ml PBS, 30 min, washed in PBS and incubated in 30 ug protK/ml PB S with 0.1% Triton X-100, 20 min, at room temper-

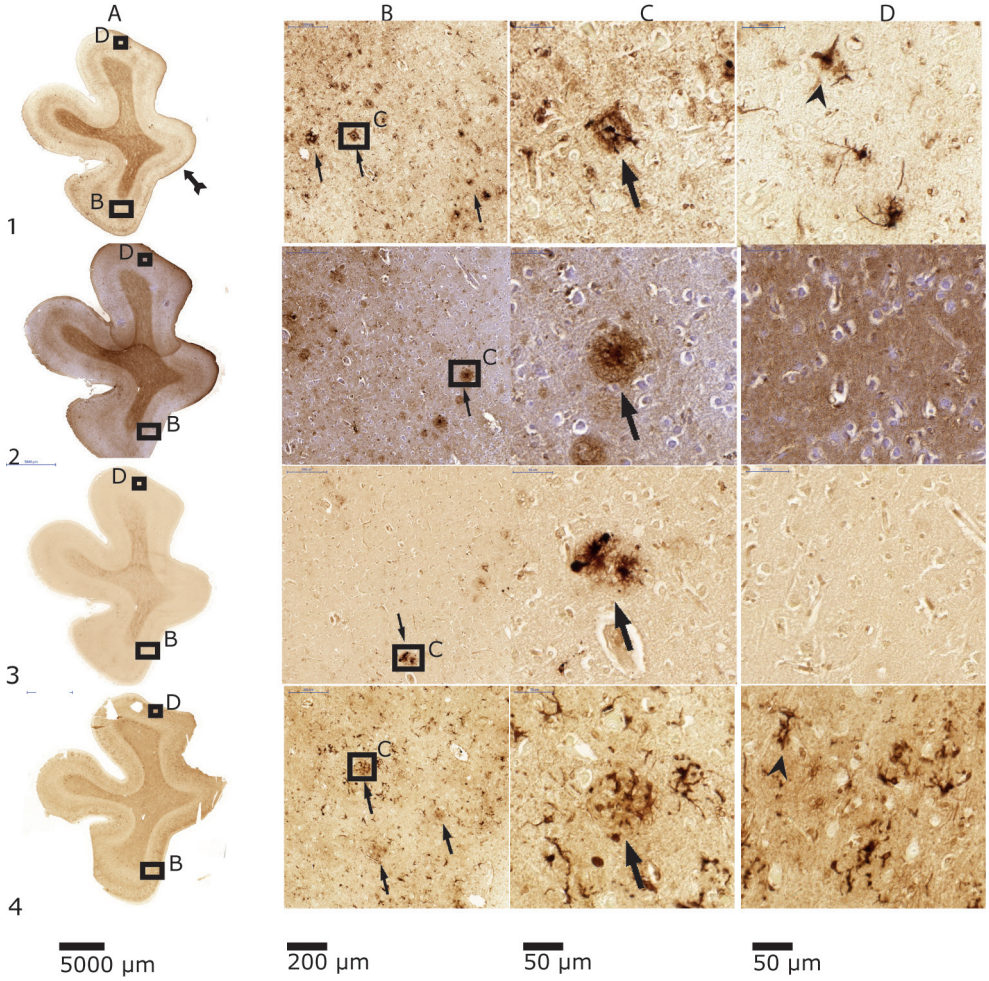

Figure 2: Comparison of the Meguro (1), Smith (2), LeVine (3) to ferritin IHC (4) on AD tissue. A: whole section (scale bar 5000 µm); B: 10x magnification (scale bar 200 µm); C: 40x magnification of 2 (scale bar 50 µm); D: 40x magnification (scale bar 50 µm). Arrows indicate examples of iron positive plaques; arrowheads indicate examples of microglia; double arrows show layer IV/V of the cortex.

ature. Sections were washed in PBS and incubated in 1% potassium ferrocyanide/1% Triton X-100/0.125 N HCL, 30 min. Sections were washed in PBS and incubated in a mixture of 1 mg DAB: 5 ml 0.01M Tris HCl pH 7.6: 10 ul 30% H2O2 for 2 hours in the dark followed by washing in PBS. The seventh section was stained immunohistochemically for ferritin using polyclonal anti-ferritin rabbit antibody at 1:10000 (Bethyl, Montgomery, Texas, USA) overnight, followed by a swine anti-rabbit biotin (Dako) 1:600 for 1 hour at room temperature. After washing with PBS, immunolabelling

followed using an ABC kit (Vectastain) according to the manufacturer's instructions and visualized with DAB (3'3 diaminobenzidine, Sigma). The concentration of ferritin rabbit antibody 1:10000 was chosen after a series of 7 different concentrations. 1:100, 1:500, 1:1000, 1:5000, 1:10000, 1:20000, 1:40000. The dilution of 1:10000 gave the most optimal signal compared to the higher and lower concentrations.
In the second experiment the three different methods and the ferritin IHC were performed on tissue of AD patients and on tissue of control patients. The tissue was cut in 10 µm thick sections and mounted onto slides. Adjacent sections were stained with the Meguro, Smith and LeVine method and the ferritin IHC as described above.

Scoring
All sections were scored for iron/ferritin labelling of plaques, microglia, white matter and cortical layers IV and V. Microglia cells were defined as iron positive cells with dilated cell bodies and dilated cellular processes. We and others have shown that iron positive cells with this morphology label for microglial immunohistochemical markers (Nabuurs et al. 2011; Schonberg et al. 2012). The intensity of iron and ferritin staining in plaques and microglia was scored as: no staining (-), intermediate staining (+) or strong staining (++). Labelling of myelin-associated iron in the white matter and the myelin rich cortical layers IV and V was scored as no contrast (-), intermediate contrast (+) and strong contrast (++) versus the rest of the cortex. Scoring was performed independently by the authors (SvD, SGvD,RN).

Results

Iron histochemistry.
The Meguro method showed the strongest contrast between gray and white matter in AD and control tissue (fig 1 and 2). This contrast was also seen using the Smith and LeVine staining, however, it was less pronounced. Cortical layers IV and V showed the most intense labelling by the Meguro stain, and labelling of these layers was more pronounced in AD than in controls. These layers were also seen to a lesser extent in the Smith staining but not in the LeVine staining. Iron-containing plaques and microglia in AD tissue were most frequently and most intensely labelled by the Meguro stain. The Smith method detected less microglia and fewer iron containing plaques in the cortices of AD patients. The LeVine meth-

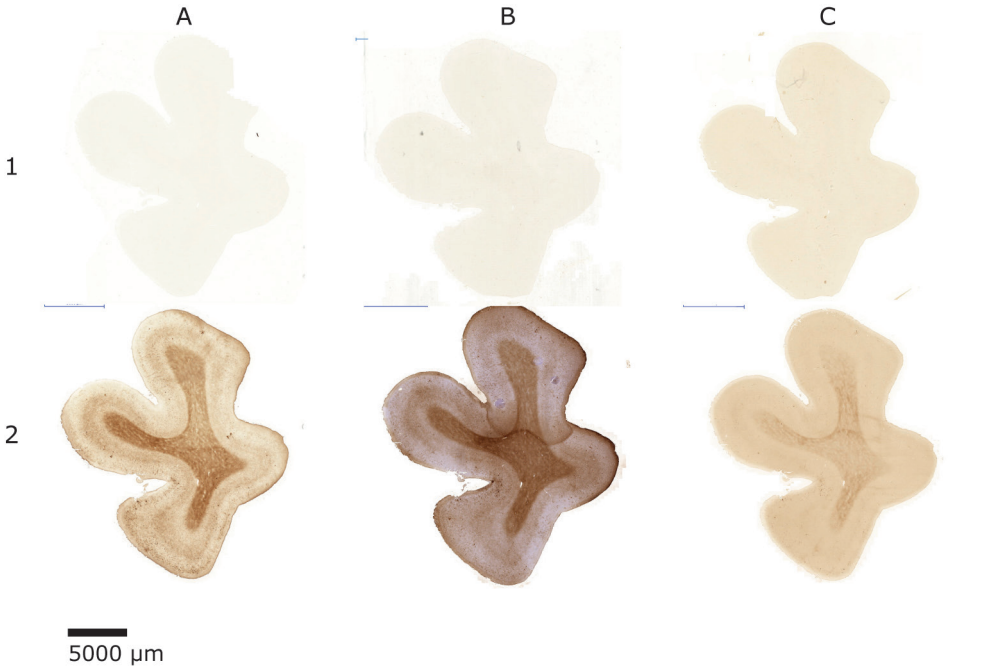

Figure 3: The Meguro (A), Smith (B), LeVine (C) method with iron extraction as pre-treatment (1) and without iron extraction as pre-treatment (2) on AD tissue; scale bars 5000 µm.

od was clearly the least sensitive, showing no enhanced labelling of the cortical layers IV/V, only a few plaques and no microglia. No iron positive plaques or microglia were found, with any of the iron staining methods, in control tissue.

Comparison with ferritin IHC

The Meguro method and ferritin IHC showed a comparable distribution and frequency of iron-positive plaques and microglia in AD tissue but the plaques looked different. Both methods showed plaques with clustered iron positive microglia, but the extracellular parenchymal plaque deposits were labelled differently. The Meguro method showed intense and sharply circumscribed labelling of extracellular plaque deposits, whereas ferritin IHC showed weak, diffuse labelling of these deposits (fig 2). The contrast between white matter and cortex and the visibility of cortical layers IV/V was better using the Meguro iron stain than in ferritin IHC in both AD tissue and control tissue. Higher concentrations of the antibody gave more background with less contrast between the different layers in the cortex and between white and grey matter.

Table 1: Comparison of LeVine, Smith, Meguro iron stain and ferritin Immunohistochemistry.

	Plaques	Microglia	Layer IV/V AD tissue	White matter AD tissue	Layer IV/V control tissue	White matter control tissue
Meguro	+/++	++	+++	++	++	+++
Smith	+	+	+	+	++	+
LeVine	+	-	-	+	-	+
Ferritin	+/++	++	+	+	+	+

Each score represents the aggregated result of the 4 patients. For iron positive plaques and microglia: - = no staining; + = intermediate staining; ++ = strong staining. For contrast between cortical layers IV/V and the other cortical layers and for contrast between white and grey matter: - = no contrast; + = intermediate contrast; ++ = strong contrast.

Iron extraction

None of the three investigated procedures showed staining of any cell or structure in tissue after iron extraction (fig 3), but all showed their usual staining pattern in the parallel section without iron extraction as a pre-treatment. Only the LeVine method showed a light background staining and lacked contrast between white matter and grey matter.

The buffer incubated with tissue showed much higher iron concentrations, than buffer incubated on a glass slide without tissue, confirming iron extraction (table 2).

Iron extraction with Na-citrate/HCL buffer gave better results compared with the TRIS/HCL buffer on the tissue. However, after adding Fe3+ to the buffer the results were better using TRIS/HCL as a buffer.

Discussion

To our knowledge, this is the first study to provide a direct comparison of three frequently used histochemical iron stains on human paraffin-embedded AD brain tissue and simultaneously investigates changes in the distribution of ferritin. We evaluated their ability to stain iron-containing plaques and microglia as well as myelin-associated iron. The method according to Meguro et al. (Meguro et al. 2007) resulted in the most robust and intense labelling of these iron containing structures.

We are not aware of earlier studies using the Meguro method to visualize iron in human brain tissue, but it has been described for the detection of iron in paraffin-embedded tissue of rat, mice, monkey and guinea pig (Meguro et al. 2005; Freret et al. 2008; Iwatsuki et al. 2008; Meguro et al. 2008; Butt et al. 2010; Winter et al. 2010; Butt et al. 2011; Shpyleva et al. 2011).

The Smith method (Smith et al. 1997) showed moderate amounts of microglia and plaques with less intensity than the Meguro stain. The staining of cortical layers IV and V was weak. With this method plaques have been demonstrated on 6 to 8 µm paraffin sections (Smith et al. 1997;van Duijn et al. 2011). Labelling of iron in microglia has not been described in earlier reports. This method differs to that described by Meguro et al. in its exclusion of the methanol-NaN3-H2O2 treatment step between the ferrocyanide and DAB amplification step as well as the much longer (overnight versus 30 minutes) incubation time, with a 7 fold higher concentration of ferrocyanide and a shorter incubation with DAB in a 3x higher concentration. How these differences result in a less intense labelling of iron-positive structures than that by the Meguro method remains unclear. For the protocol used by Smith et al. methacarn fixation has been described to result in better iron labelling than formalin fixation. We performed the Smith protocol on formalin-fixed tissue because in our and most other laboratories tissue is routinely fixed by formalin; thus a general iron staining should be optimized preferably for formalin fixed tissue.

The last technique, published by LeVine (LeVine 1991), showed the least intense staining of the scored characteristics or no staining at all. Earlier studies showed plaques using this method on 60- to 100-µm free-floating sections (LeVine 1997; Meadowcroft et al. 2009) and iron-containing microglia in multiple sclerosis brains (LeVine 1997). No results of iron in layers IV/V have been reported using this method. The most likely explanation for the inferior labelling of plaques in the LeVine method compared to the other stains is our use of 10-µm de-paraffinized sections on glass slides whereas the LeVine method has been developed for 60- to 100-µm free-floating sections (LeVine 1991; LeVine et al. 1992; LeVine et al. 1993). The absence of labelling of cortical layers IV and V may be due to the aggressive pre-treatment releasing iron from the myelin which is slightly increased compared to the other layers.

Table 2: quantification of iron present in the extraction buffer after incubation;

	Fe (µmol/L)	
	Na-citrate	TRIS/HCL
Patient 1	4,7	2,3
Patient 2	5,3	1,7
Patient 3	4,7	2,3
Patient 4	4,4	1,7
Slide without tissue	1,5	0,9
Native buffer	0,9	0,9
Buffer + 10 µg Fe^{3+}/ml	191,9	217,4
Buffer + 1 µg Fe^{3+}/ml	20,1	20,9
Buffer + 0,1 µg Fe^{3+}/ml	3,1	2,9

These results were not corrected for the amount of tissue that was incubated.

Using the Meguro technique, the contrast between white and grey matter and between cortical layers IV/V and the other cortical layers was more intense than using ferritin IHC. This may be due to problems with antigen retrieval in myelin-containing tissue. A problem of antibody sensitivity seems unlikely because intracellular microglial staining is very strong and frequent in ferritin IHC, similar to that observed with the Meguro iron stain. The differences between the Meguro iron stain and the ferritin IHC remained when higher or lower ferritin antibody concentrations were used. Alternatively, there may be a true difference between the presence of iron and ferritin in myelin due to a relatively high non-ferritin bound iron pool in the white matter and in cortical layers IV/V. Oligodendrocyte differentiation from oligodendrocyte precursor cells and myelin synthesis requires high iron concentrations, presumably because high amounts of enzymes with iron at their active sites are necessary (Todorich et al. 2009). The different labelling of plaques by the Meguro method and ferritin IHC is possibly caused by binding of iron to some of the many molecules other than ferritin in the extracellular compartment of plaques (Grundke-Iqbal et al. 1990; Connor et al. 1995).

The specificity of the tested histochemical iron stains was checked by using sections depleted of iron in acid buffer as a negative control. The absence of iron staining in these iron-depleted sections confirms the results of another study using the Smith protocol on iron depleted sections (Smith et al., 2007). Staining of other metals in brain is not completely excluded by these experiments, but other studies report the absence of DAB oxidation in reaction products of ferrocyanide with copper, zinc or magnesium (Meguro et al., 2007; Meguro et al. 2003; Roschzttardtz et al. 2009). All this information supports that the modified, DAB enhanced Perl's stainings used in this study are specific for iron ions.

Detailed knowledge of iron distribution in brain tissue may be of value for improving in vivo (MRI) diagnostics in AD and for a more complete picture of the pathogenesis of AD. In addition, it may also reflect normal brain ageing (Bartzokis et al. 2007b; Pfefferbaum et al. 2010) and the presence of other neurodegenerative diseases such as Parkinson's disease (Loeffler et al. 1995; Brar et al. 2009), Lewy body disease (Tuite et al. 1996; Golts et al. 2002) and Huntington's disease (Bartzokis et al. 2007a; Rosas et al. 2012). Although the present study was done on AD brain tissue, the results may be of use for the choice of iron stain in these other neurode-

generative diseases.
In conclusion, the results of this study suggest that the Meguro method is the best technique to stain iron in 10-μm formalin fixed paraffin sections of human brain tissue. Ferritin IHC is a good alternative for demonstrating iron in microglia and, to a lesser amount, plaques, but somewhat less suitable for staining myelin-associated iron.

Acknowledgment
The authors thank I. Hegeman-Kleinn for her excellent technical assistance.

Reference List

Barbeito, A.G., Garringer, H.J., Baraibar, M.A., Gao, X.Y., Arredondo, M., Nunez, M.T., Smith, M.A., Ghetti, B., & Vidal, R. 2009. Abnormal iron metabolism and oxidative stress in mice expressing a mutant form of the ferritin light polypeptide gene. Journal of Neurochemistry, 109, (4) 1067-1078

Bartzokis, G. 2011. Alzheimer's disease as homeostatic responses to age-related myelin breakdown. Neurobiol.Aging, 32, (8) 1341-1371

Bartzokis, G., Lu, P.H., Tishler, T.A., Fong, S.M., Oluwadara, B., Finn, J.P., Huang, D., Bordelon, Y., Mintz, J., & Perlman, S. 2007a. Myelin breakdown and iron changes in Huntington's disease: pathogenesis and treatment implications. Neurochem. Res., 32, (10) 1655-1664

Bartzokis, G., Tishler, T.A., Lu, P.H., Villablanca, P., Altshuler, L.L., Carter, M., Huang, D., Edwards, N., & Mintz, J. 2007b. Brain ferritin iron may influence age- and gender-related risks of neurodegeneration. Neurobiol. Aging, 28, (3) 414-423

Brar, S., Henderson, D., Schenck, J., & Zimmerman, E.A. 2009. Iron accumulation in the substantia nigra of patients with Alzheimer disease and Parkinsonism. Archives of Neurology, 66, (3) 371-374

Butt, O.I., Buehler, P.W., & D'Agnillo, F. 2010. Differential induction of renal heme oxygenase and ferritin in ascorbate and nonascorbate producing species transfused with modified cell-free haemoglobin. Antioxidants & Redox Signaling, 12, (2) 199-208

Butt, O.I., Buehler, P.W., & D'Agnillo, F. 2011. Blood-brain barrier disruption and oxidative stress in guinea pig after systemic exposure to modified cell-free haemoglobin. American Journal of Pathology, 178, (3) 1316-1328

Chen-Roetling, J., Chen, L.F., & Regan, R.F. 2011. Apotransferrin protects cortical neurons from haemoglobin toxicity. Neuropharmacology, 60, (2-3) 423-431

Connor, J.R., Snyder, B.S., Arosio, P., Loeffler, D.A., & Lewitt, P. 1995. A

quantitative-analysis of isoferritins in select regions of aged, parkinsonian, and, Alzheimers diseased brains. Journal of Neurochemistry, 65, (2) 717-724

Crichton, R.R., Wilmet, S., Legssyer, R., & Ward, R.J. 2002. Molecular and cellular mechanisms of iron homeostasis and toxicity in mammalian cells. J. Inorg. Biochem., 91, (1) 9-18

Fatterpekar, G.M., Naidich, T.P., Delman, B.N., Aguinaldo, J.G., Gultekin, S.H., Sherwood, C.C., Hof, P.R., Drayer, B.P., & Fayad, Z.A. 2002. Cytoarchitecture of the human cerebral cortex: MR microscopy of excised specimens at 9.4 Tesla. AJNR Am. J. Neuroradiol., 23, (8) 1313-1321

Freret, T., Bouet, V., Toutain, J., Saulnier, R., Pro-Sistiaga, P., Bihel, E., MacKenzie, E.T., Roussel, S., Schumann-Bard, P., & Touzani, O. 2008. Intraluminal thread model of focal stroke in the non-human primate. Journal of Cerebral Blood Flow and Metabolism, 28, (4) 786-796

Fukunaga, M., Li, T.Q., van, G.P., de Zwart, J.A., Shmueli, K., Yao, B., Lee, J., Maric, D., Aronova, M.A., Zhang, G., Leapman, R.D., Schenck, J.F., Merkle, H., & Duyn, J.H. 2010. Layer-specific variation of iron content in cerebral cortex as a source of MRI contrast. Proc. Natl. Acad. Sci. U.S.A, 107, (8) 3834-3839

Golts, N., Snyder, H., Frasier, M., Theisler, C., Choi, P., & Wolozin, B. 2002. Magnesium inhibits spontaneous and iron-induced aggregation of alpha-synuclein. Journal of Biological Chemistry, 277, (18) 16116-16123

Grundke-Iqbal, I., Fleming, J., Tung, Y.C., Lassmann, H., Iqbal, K., & Joshi, J.G. 1990. Ferritin is a component of the neuritic (senile) plaque in Alzheimer dementia. Acta Neuropathol., 81, (2) 105-110

Haacke, E.M., Cheng, N.Y., House, M.J., Liu, Q., Neelavalli, J., Ogg, R.J., Khan, A., Ayaz, M., Kirsch, W., & Obenaus, A. 2005. Imaging iron stores in the brain using magnetic resonance imaging. Magn Reson. Imaging, 23, (1) 1-25

Iwatsuki, H., Meguro, R., Asano, Y., Odagiri, S., Li, C.T., & Shoumura, K. 2008. Chelatable Fe (II) is generated in the rat kidneys exposed to is-

chemia and reperfusion, and a divalent metal chelator, 2, 2 '-dipyridyl, attenuates the acute ischemia/reperfusion-injury of the kidneys: a histochemical study by the perfusion-Perls and -Turnbull methods. Archives of Histology and Cytology, 71, (2) 101-114

LeVine, S.M. 1991. Oligodendrocytes and myelin sheaths in normal, quaking and shiverer brains are enriched in iron. J. Neurosci. Res., 29, (3) 413-419

LeVine, S.M. 1997. Iron deposits in multiple sclerosis and Alzheimer's disease brains. Brain Research, 760, (1-2) 298-303

LeVine, S.M. & Torres, M.V. 1992. Morphological features of degenerating oligodendrocytes in twitcher mice. Brain Research, 587, (2) 348-352

LeVine, S.M. & Torres, M.V. 1993. Satellite oligodendrocytes and myelin are displaced in the cortex of the reeler mouse. Developmental Brain Research, 75, (2) 279-284

Loeffler, D.A., Connor, J.R., Juneau, P.L., Snyder, B.S., Kanaley, L., Demaggio, A.J., Nguyen, H., Brickman, C.M., & Lewitt, P.A. 1995. Transferrin and iron in normal, Alzheimers disease, and Parkinsons disease brain regions. Journal of Neurochemistry, 65, (2) 710-716

Meadowcroft, M.D., Connor, J.R., Smith, M.B., & Yang, Q.X. 2009. MRI and histological analysis of beta-amyloid plaques in both human Alzheimer's disease and APP/PS1 transgenic mice. Journal of Magnetic Resonance Imaging, 29, (5) 997-1007

Meguro, R., Asano, Y., Iwatsuki, H., & Shoumura, K. 2003. Perfusion-Perls and –Turnbull methods supplemented by DAB intensification for nonheme iron histochemistry: demonstration of the superior sensitivity of the methods in the liver, spleen, and stomach of the rat. Histochem. Cell Biol., 120, (1) 73-82

Meguro, R., Asano, Y., Odagiri, S., Li, C., Iwatsuki, H., & Shoumura, K. 2005. The presence of ferric and ferrous iron in the nonheme iron store of resident macrophages in different tissues and organs: histochemical demonstrations by the perfusion-Perls and -Turnbull methods in the rat.

Arch. Histol. Cytol., 68, (3) 171-183

Meguro, R., Asano, Y., Odagiri, S., Li, C., Iwatsuki, H., & Shoumura, K. 2007. Nonheme-iron histochemistry for light and electron microscopy: a historical, theoretical and technical review. Arch. Histol. Cytol., 70, (1) 1-19

Meguro, R., Asano, Y., Odagiri, S., Li, C.T., & Shoumura, K. 2008. Cellular and subcellular localizations of nonheme ferric and ferrous iron in the rat brain: a light and electron microscopic study by the perfusion-Perls and -Turnbull methods. Archives of Histology and Cytology, 71, (4) 205-222

Nabuurs, R.J., Hegeman, I., Natte, R., van Duinen, S.G., van Buchem, M.A., van der Weerd, L., & Webb, A.G. 2011. High-field MRI of single histological slices using an inductively coupled, self-resonant microcoil: application to ex vivo samples of patients with Alzheimer's disease. NMR Biomed., 24, (4) 351-357

Nabuurs, R. J. A., van Rooden, S., van Duijn, S., Versluis, M. J., Emmer, B. J., Liem, M. K., Milles, J. R. R, Webb, A., Frosch, M.,van Duinen, S., Natte, R., van der Grond, J., van der Weerd, L., & van Buchem, M. A. 2013. Cortical changes in Alzheimer's disease at ultra-high field MRI. Submitted

Pfefferbaum, A., Adalsteinsson, E., Rohlfing, T., & Sullivan, E.V. 2010. Diffusion tensor imaging of deep gray matter brain structures: effects of age and iron concentration. Neurobiol.Aging, 31, (3) 482-493

Rosas, H.D., Chen, Y.I., Doros, G., Salat, D.H., Chen, N.K., Kwong, K.K., Bush, A., Fox, J., & Hersch, S.M. 2012. Alterations in brain transition metals in Huntington disease: an evolving and intricate story. Arch. Neurol., 69, (7) 887-893

Roschzttardtz H., Conéjéro G., Curie C., Mari S. 2009. Identification of the endodermal vacuole as the iron storage compartment in the arabidopsis embryo. Plant Physiology, 151, 1329-1338

Schonberg, D.L., Goldstein, E.Z., Sahinkaya, F.R., Wei, P., Popovich, P.G., & McTigue, D.M. 2012. Ferritin stimulates oligodendrocyte genesis in the adult spinal cord and can be transferred from macrophages to NG2 cells

in vivo. Journal of Neuroscience, 32, (16) 5374-5384

Shpyleva, S.I., Muskhelishvili, L., Tryndyak, V.P., Koturbash, I., Tokar, E.J., Waalkes, M.P., Beland, F.A., & Pogribny, I.P. 2011. Chronic administration of 2-acetylaminofluorene alters the cellular iron metabolism in rat liver. Toxicological Sciences, 123, (2) 433-440

Smith, K.D., Kallhoff, V., Zheng, H., & Pautler, R.G. 2007. In vivo axonal transport rates decrease in a mouse model of Alzheimer's disease. Neuroimage., 35, (4) 1401-1408

Smith, M.A., Harris, P.L., Sayre, L.M., & Perry, G. 1997. Iron accumulation in Alzheimer disease is a source of redox-generated free radicals. Proc. Natl. Acad. Sci. U.S.A, 94, (18) 9866-9868

Todorich, B., Pasquini, J.M., Garcia, C.I., Paez, P.M., & Connor, J.R. 2009. Oligodendrocytes and myelination: the role of iron. Glia, 57, (5) 467-478

Tuite, P.J., Provias, J.P., & Lang, A.E. 1996. Atypical dopa responsive parkinsonism in a patient with megalencephaly, mid-brain Lewy body disease, and some pathological features of Hallervorden-Spatz disease. Journal of Neurology Neurosurgery and Psychiatry, 61, (5) 523-527

van Duijn, S., Nabuurs, R.J., van, R.S., Maat-Schieman, M.L., van Duinen, S.G., van Buchem, M.A., van der Weerd, L., & Natte, R. 2011. MRI artifacts in human brain tissue after prolonged formalin storage. Magn Reson. Med., 65, (6) 1750-1758

Winter, E.M., Hogers, B., van der Graaf, L.M., Gittenberger-de Groot, A.C., Poelmann, R.E., & van der Weerd, L. 2010. Cell tracking using iron oxide fails to distinguish dead from living transplanted cells in the infarcted heart. Magnetic Resonance in Medicine, 63, (3) 817-821